ACS Catalysis

pubs.acs.org/acscatalysis
Research Article

Electrocatalysis of Oxygen Reduction on Te-Modified Platinum Stepped Crystal Surfaces

Ting-Ting Mao, Zhen Wei, Bing-Yu Liu, Yu-Jun Xu, Jun Cai, Yan-Xia Chen,* Juan M. Feliu, and Enrique Herrero*

Cite This: ACS Catal. 2023, 13, 16045−16054
Read Online

ACCESS | Metrics & More | Article Recommendations | Supporting Information

ABSTRACT: Te-modified platinum single-crystal surfaces in the [01$\bar{1}$] zone have been used as model electrocatalysts for oxygen reduction reaction (ORR). The results clearly show that (1) except for Pt(111), all other electrodes display enhanced ORR activity when Te is deposited on the surface; (2) the intrinsic ORR activity for Pt(*hkl*) decreases in the order of Pt(322) > Pt(755) > Pt(977) > Pt(111) > Pt(311) > Pt(100), while the enhancement factor for ORR with Te modification decreases in the order of Pt(100) > Pt(311) > Pt(977) > Pt(755) > Pt(322); (3) metallic Te and its charge transfer to Pt as well as the consequent lower d-band center and OH_{ad} binding energy are probably the reasons for the enhanced electrocatalysis for ORR with Te modification; and (4) the inhibition of Te at Pt(111) as well as the smaller extent for the enhancement of Te at Pt(S)-[*n*(111) × (100)] with longer terraces in the kinetic region for ORR are a result of partial oxidation of Te. The weaker electronic interaction of Te with the Pt substrate is probably the origin of its facile oxidation at lower potential. Our results imply that modification of Pt with species that can transfer electrons to Pt may be an efficient strategy to enhance the ORR activity.

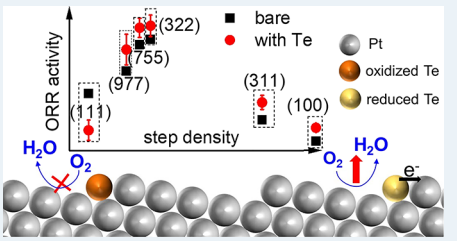

KEYWORDS: *oxygen reduction reaction, platinum stepped crystal planes, Te modification, electron transfer, OH_{ad} binding energy*

1. INTRODUCTION

Polymer electrolyte membrane fuel cells (PEMFCs) are promising technologies for the extensive use of sustainable energy due to their high energy conversion efficiency and the wide range of potential applications with different power density scales.[1−3] However, the high overpotential of oxygen reduction reaction (ORR) at the cathode of PEMFCs requires a high loading of precious Pt group catalysts which limits large-scale application.[4,5] Thus, developing cathode catalysts with high electrocatalytic activity is of significant importance.[6] For that, it is necessary to understand the ORR mechanism and factors that affect ORR kinetics on the electrocatalysts.[7] However, the complex catalyst structure in practical electrode materials limits the in-depth study of ORR kinetics.[8−10] Single-crystal electrodes with well-defined surfaces and a controlled atomic arrangement[11−18] are of great help in elucidating the reaction mechanism and unraveling the structure−activity relationship. Systematic studies of the platinum stepped surfaces with different terrace widths have provided rich information, such as the chemical properties of the electrode/electrolyte interface at the atomic level and how these properties affect its behavior.[19−21] The information gained from such studies has shed important insights into real electrocatalysts in PEMFCs.[22−24]

Recently, the chemical modification of the model electrode surfaces by foreign metals with special electronic properties has been shown to significantly alter their electrocatalytic behavior.[25−32] The electrocatalytic properties of platinum single-crystal electrodes modified by underpotential deposition (UPD)[33,34] and chemical adsorption/deposition of other foreign adatoms have been widely investigated and discussed,[35−37] especially in the field of electrocatalytic oxidation of small organic molecules, such as glycerol,[38] formic acid,[39,40] and ethanol.[41,42] Spontaneous adsorption of foreign atoms such as tellurium, sulfur, bismuth, and selenium on the Pt(*hkl*) electrode surface upon immersion has proven to be a useful method for constructing the modified model electrocatalysts.[43,44] Moreover, information gained through modification has been successfully employed for the rational design of nanocatalysts with improved reactivity for electrochemical energy substance conversion devices including PEMFCs.[45−49] Recently, studies have reported that the oxygen reduction reaction activity on platinum single-crystal electrodes and nanoparticles can be substantially improved by the adsorption of metals,[27,50,51] amines,[52,53] hydrophobic cations,[54] ionic liquids,[55] and melamine.[56,57] Nevertheless, studies on the modification of Pt(*hkl*) by oxygen group elements (VIA group) such as tellurium and their ORR performance are rare. A preliminary study by Feliu and co-workers found that Te

Received: October 12, 2023
Revised: November 9, 2023
Accepted: November 21, 2023

https://doi.org/10.1021/acscatal.3c04876
ACS Catal. 2023, 13, 16045−16054

modification of Pt(111) hampered the ORR performance.[58] To gain a comprehensive understanding of how Te modification changes the electrode surface properties, this study extends the research of the ORR behavior to Te-modified Pt(100) and a series of platinum stepped surfaces (Pt(S)-[n(111) × (100)]). Significant enhancement of ORR performance at the Te-modified Pt(S)-[n(111) × (100)] is observed, and the enhancement factor for ORR with Te modification is found to decrease in the order Pt(100) > Pt(311) > Pt(977) > Pt(755) > Pt(322). The mechanism for the enhancement with Te, including how it tunes the electron distribution,[59] atomic arrangements, and binding energies of the reaction intermediates for ORR, will be discussed.

2. EXPERIMENTAL SECTION

The platinum single-crystal electrodes used in the experiment were prepared by melting the end of the platinum wire (Φ = 0.5 mm) using H_2/O_2 flame to form platinum beads with a diameter of 2−3 mm following Clavier's method.[11] The Pt beads were oriented using the diffraction spots obtained with a laser, followed by cutting and polishing steps to expose the desired planes in the $[01\bar{1}]$ crystallographic region. This region contains surfaces with n atom-wide (111) terraces and (100) monatomic steps. Prior to all experiments, the platinum single-crystal electrodes were annealed by inductive heating at 370 A for 60 s (the selected current depends on the diameter of the Pt electrodes) and then completely cooled in a reductive atmosphere with Ar/CO (9:1) and transferred into ultrapure water saturated with Ar/CO gas mixture. After that, the platinum electrode was covered by a droplet of water, which protected it from impurities in the air. Solutions were prepared using perchloric acid (Aladdin, AR), TeO_2 (Sigma-Aldrich), ultrapure water (18.2 MΩ cm, from Milli-Q water system), and Ar, O_2, and Ar/CO gas mixture with a purity of 99.99% purchased from Nanjing Shang yuan Industrial Gas Company.

The electrode potentials were controlled with a potentiostat (Autolab 302N). Cyclic voltammetry (CV) experiments were carried out at room temperature in a three-electrode all-glass cell, which is equipped with a Pt wire as the counter electrode and a Ag/AgCl electrode as the reference electrode. All potentials used here are quoted against a reversible hydrogen electrode (RHE) scale. For the preparation of Te-modified platinum single-crystal electrodes, a freshly annealed electrode was immersed in 0.1 M $HClO_4$ + 10^{-5}−10^{-7} M TeO_2 solution for 5−30 s, during which Te could spontaneously adsorb on the Pt electrode surface. To obtain different coverages of Te adsorbed on the Pt(hkl) electrodes, the concentration of the Te solution or the immersion time could be changed. Afterward, the prepared Te-modified Pt(hkl) electrode (denoted as Pt(hkl)@Te) was rinsed with large amounts of ultrapure water to remove any Te species that were not adsorbed on the surface. Finally, the Pt(hkl)@Te electrode was characterized in Ar-saturated 0.1 M $HClO_4$. The activity of the oxygen reduction reaction (ORR) was measured in an O_2-saturated 0.1 M $HClO_4$ using the hanging meniscus rotating disk electrode (HMRDE) configuration. For the case of the ORR in O_2-saturated 0.1 M $HClO_4$ (pH = 1.2), the typical iR drop[60] (which depends on the meniscus height) was ca. 100 Ω. Here, 90% ohmic compensation (90 Ω) was carried out during all ORR processes. The deposition of Te on the electrode was removed by immersion in concentrated nitric acid solution for 5−10 s. Then, the electrode was anneales to obtain a well-defined surface.

3. RESULTS AND DISCUSSION

3.1. Voltammetric Behavior of Te-Modified Pt(100) Electrodes. Figure 1 shows the different cyclic voltammograms (CVs) of the Te-modified Pt(100) electrodes in 0.1 M $HClO_4$. As can be seen, the CV of the unmodified Pt(100) surface agrees with that reported in the literature,[61,62] which confirms the quality of the electrodes used in this study. Starting from 0.06 V, where the surface is completely covered by adsorbed hydrogen, hydrogen initially desorbs at the defect sites of the Pt(100) electrode. This results in a small peak at about 0.3 V. Then, the broader peak around 0.38 V corresponds to hydrogen (H) desorption on the well-ordered (100) domains. Notably, the peak height ratios between 0.38 and 0.3 V are indicative of the electrode quality. Subsequently, hydroxyl (OH) adsorption occurs on the Pt(100) surface between 0.45 and 0.7 V.[63]

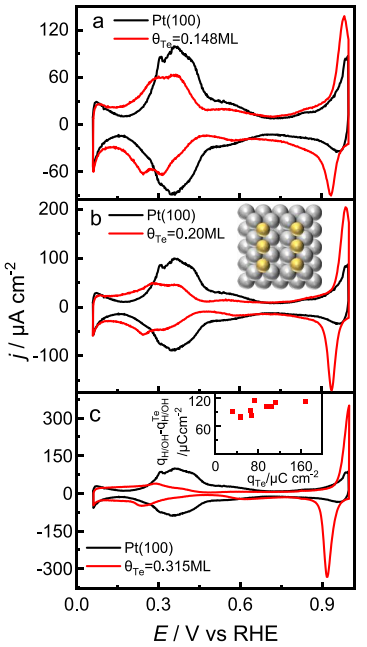

Figure 1. Cyclic voltammograms of Te-modified Pt(100) with different coverages in Ar-saturated 0.1 M $HClO_4$. The inset in (b) shows the adsorption model for Te on Pt(100) at the 4-fold sites. The inset in (c) shows the plot of the charge difference between the unmodified electrode and the Te-modified electrodes from 0.06 to 0.75 V vs the charge of the redox process of Te adatoms. Scan rate: 50 mV/s. Potential region: 0.06−1.0 V.

For Te-modified Pt(100) electrodes, the CVs change significantly compared with the unmodified electrode. The decrease in the charge density under the hydrogen and hydroxyl regions is apparent. In fact, the signals corresponding to adsorbed hydrogen move to lower potential values and those relating to adsorbed OH shift to higher values, indicating that both processes are weaker on the Te-modified Pt(100) surface. Furthermore, a new peak at ca. 0.93−0.95 V appears,[64] corresponding to the redox process on Te adatoms (eq 1) previously reported[58]:

$$\mathrm{Pt(100)-TeO_{2(ads)} + 4H^+_{(aq)} + 4e^-} \leftrightarrow \mathrm{Pt(100)-Te_{(ads)} + 2H_2O} \quad (1)$$

https://doi.org/10.1021/acscatal.3c04876
ACS Catal. 2023, 13, 16045−16054

The asymmetric oxidation and reduction peaks suggest that the process occurring on Te is irreversible. DFT calculations of the adsorption energy of Te on Pt(100) surfaces indicate that the most favorable adsorption site is the 4-fold hollow site shown in the inset of Figure 1b.[65] To calculate the Te coverage, we used the adsorption charges on the modified and unmodified electrodes. It should be highlighted that the charge density for the adsorption−desorption processes on the Te-modified Pt(100) electrode was calculated as the integral area between 0.06 and 0.75 V after subtraction of the apparent double layer. This charge comprises the contributions for the hydrogen and hydroxyl adsorption/desorption processes, which cannot be separated. According to the redox process in eq 1 and DFT calculations, a Te adatom on the (100) surface occupies 4-fold hollow sites and exchanges 4 electrons in the redox process. Using this stoichiometry, the maximum Te coverage is estimated to be 0.5 ML.[64] However, the maximum coverage of Te that can be obtained experimentally is about 0.35 ML, which may be attributed to the lateral interaction of Te adsorbed on Pt(100). Thus, the coverage can be calculated as

$$\theta_{Te} = \frac{q_{H/OH} - q^{Te}_{H/OH}}{2 \times q_{H/OH}} \quad (2)$$

where $q_{H/OH}$ and $q^{Te}_{H/OH}$ are the integrated charge between 0.06 and 0.75 V for the unmodified and Te-modified Pt(100) electrodes, respectively. Unlike what is observed for the Te-modified Pt(111) electrode (Figure S2a), there is no linear relationship between the charge density of the Te (q_{Te}) redox process and the charge for the H/OH adsorption/desorption processes on the Pt(100) surface(inset of Figure 1c). This result can be a consequence of Te on the Pt(100) electrode not just acting as a pure third-body but having an electronic effect, which modifies the H_{ad} and OH_{ad} properties at Pt(100) and induces changes in the surface catalytic properties. This is also supported by the negative and positive shifts of the current wave for H_{ad} and OH_{ad} (Figure 1), respectively.

Figure 2 shows the ORR polarization curves obtained on Te-modified Pt(100) electrodes with different Te coverages. The whole set of figures at different rotation rates is shown in Figure S1a,b. In all cases, diffusion-limiting plateaus are explicitly seen in the potential range of 0.3−0.6 V. The diffusion-limiting current, j_L, obeys the Levich equation:

$$j_L = -0.62nFD^{2/3}\nu^{-1/6}c_b\omega^{1/2} \quad (3)$$

where n is the number of transferred electrons for the ORR, F is the Faraday constant, 96,485 C mol^{-1}, D is the diffusion constant, ν is the solution viscosity, c_b is the bulk concentration of reactants, and ω is the rotation rate. This expression has been deduced for electrodes enclosed in a protective shield. In the present case, the electrode is in the hanging meniscus configuration and the conditions are different from those of eq 3. However, it has been shown that for this type of small electrode, limiting currents are still proportional to $nFD^{2/3}\nu^{-1/6}c_b\omega^{1/2}$.[66] In this case, as shown in the insets of Figure S1, a straight line crossing the y-axis at 0 can be fitted to the different j_L vs $\omega^{1/2}$, confirming previous results. Thus, the Levich equation can be applied, and the only change from the usual expression is the 0.62 factor. Thus, the theoretical current density at 2500 rpm for the ORR according to eq 3 is −7.14 mA cm^{-2}, whereas the measured limiting current for the Pt(100) electrode is −8.2 mA cm^{-2}. It should be noted that the meniscus height slightly affects the actual value of the limiting current density. In all cases, the limiting current density is nearly the same since it depends only on the geometrical area of the electrode.

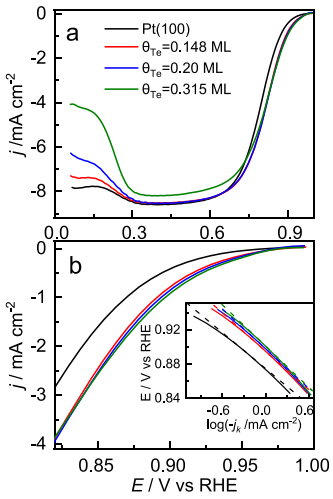

Figure 2. Linear sweep voltammograms for the ORR in hanging meniscus configuration at 2500 rpm (positive scan direction) in O_2-saturated 0.1 M $HClO_4$ for Te-modified Pt(100) electrodes with different Te coverages between (a) 0.06 and 1.0 V and (b) 0.75 and 1.0 V. The inset in (b) shows the Tafel plots for different Te coverages. Scan rate: 50 mV/s.

The value of the diffusion-limiting current allows to obtain the ORR kinetic current (j_k), which is the current that would have been obtained in the absence of the mass transfer effect as[66,67]

$$j_k = (j_L - j)/(j_L \cdot j) \quad (4)$$

where j is the measured current density at a given potential. Using this equation, the kinetic current density can be calculated. Two elements are used in this study. First, the plot of the log (j_k) vs E will allow calculating the Tafel slope, which is a parameter relevant to the ORR mechanism. On the other hand, the value of j_k (2500 rpm) at 0.9 and 0.85 V will serve for the comparison of the activity of different electrodes.

The analysis of the ORR activity for Te-modified Pt(100) electrodes reveals that the onset and half-wave potentials shift positively with increasing Te coverage (θ_{Te}) (Figure 2b), implying that Te modification enhances the ORR activity. The same conclusion is reached when j_k values are calculated (inset of Figure 2b). Additionally, the Tafel slope is around −60 mV regardless of coverage, which means that the reaction mechanism remains unchanged. On the other hand, at lower potentials (E < 0.35 V), there is a diminution in the current density for ORR, associated with the inhibition of the further reduction of hydrogen peroxide formed as an intermediate during ORR. Studies with Pt(111) electrodes and Pt stepped surfaces with (111) terraces have shown that this inhibition is linked to the electrode charge and the presence of adsorbed OH on the surface.[68,69] Thus, at potentials negative to the local potential of zero free charge (pzfc) (whose value for Pt(111) at this pH is ca. 0.33 V) and in the absence of adsorbed OH on the surface, the reduction of hydrogen peroxide is inhibited. For the Pt(100) electrode, the potential of pzfc could not be measured, but it is presumed to be located at lower values compared to that at Pt(111), based on the work function

https://doi.org/10.1021/acscatal.3c04876
ACS Catal. 2023, 13, 16045−16054

values.[70] For this reason, the extent of inhibition of hydrogen peroxide reduction on Pt(100) at 0.2 V < E < 0.3 V is lower than that on Pt(111).[71] As can be seen, the inhibition effects are more pronounced with higher Te coverage and the onset shifts toward higher potential values. It has been demonstrated that the deposition of adatoms on the Pt(111) increases the potential of maximum entropy of the interphase, which is related to the potential of zero free charge.[72,73] Consequently, as the Te coverage increases, more negative charges accumulate on the Pt sites at E < 0.2 V, leading to a larger inhibition of hydrogen peroxide reduction.

The behavior of the Te-modified Pt(111) electrodes is different. The ORR activity for the Pt(111) electrode decreases with Te coverage, as indicated by the fact that the onset and half-wave potentials shift to more negative values with Te coverage (Figure S2a,b). The difference between the behaviors of the Pt(100) and Pt(111) electrodes is related to the state of Te. For Pt(100), the potential of the redox peak for adsorbed Te is above 0.95 V, which means that adsorbed Te is always in its reduced state during the ORR process. On the other hand, the peak potential for the Te redox process on Pt(111) is ca. 0.83 V. This is in good agreement with DFT results, which show that the dipole created on the surface due to the presence of Te is larger on the Pt(111) surface than on the Pt(100) surface.[65] The larger dipole on the Pt(111) surface with the positive part on the Te adatom favors OH adsorption on the Te adatoms on the Pt(111) electrode. In a word, our results indicate that Te on Pt(111) is in its oxidized state in the mixed kinetic and mass transport potential region for ORR. Te adatoms in the oxidized state act only as spectators, that is, third-body effect, which blocks active sites and reduces the ORR activity.[58] However, a sharp increase in the ORR current can be observed at the peak potential for the redox process of Te on the Te-modified Pt(111) electrode (Figure S2b). Conversely, Te adatoms in the reduced state catalyze the ORR activity. The observed behavior of the Te-modified Pt(111) and Pt(100) electrodes implies that enhancement of the ORR depends on the substrate surface structure and the Te redox state. DFT results show that there is a charge transfer from the Te adatoms to the Pt surface.[65,74] The additional negative charge on the Pt surface results in less favorable OH adsorption on Pt, as demonstrated by the CVs in Figure 1. Since the rate-determining step (RDS) is the OH desorption step on Pt,[75] this fact activates the ORR. Recent results using D_2O show that the activity for the ORR increases when the interaction of adsorbed OD with the surface is weakened compared to that of OH.[76] However, the adsorption of OH on the Te adatoms has a negative effect on the catalytic enhancement. For the Pt(111) electrode, the peak potential for the Te redox process is lower than that on Pt(100). The presence of adsorbed OH on Te should alter the interfacial properties, as demonstrated for the Pt(111) electrode in which the presence of an adsorbed OH layer on the surface alters the surface charge. In 0.1 M $HClO_4$, the electrode surface charge is positive at the onset of OH adsorption (ca. 0.6 V) and the surface charge becomes negative as the OH layer is completed.[77] This fact implies that the structure of the interphase and especially the water adlayer is different, and thus, an impact on the ORR is expected. Thus, the positive effect for the ORR disappears when OH adsorbs on the Te adatoms because it alters the interactions between the species in the interphase (water, oxygen, and anions) and the Pt surface.

3.2. Voltammetric Behavior of Te-Modified Pt(322).

In order to better understand the effect of the Te adatoms on Pt electrodes for the ORR, Pt stepped surfaces with n atom-wide (111) terraces and (100) monatomic steps were studied. For simplicity, the discussion will focus first on the Pt(322) surface, which consists of 5 atom-wide (111) terraces separated by (100) monatomic steps. The whole set of results for the Voltammetric behavior and ORR activity of other stepped electrodes with different terrace widths can be seen in Figures S3−5. For the Voltammetric behavior of the unmodified Pt(322) electrode (Figure 3), hydrogen adsorption−desorption on the (111) terraces takes place at 0.06−0.3 V. The peak at 0.28 V is assigned to the competitive adsorption of H_{ad} and OH_{ad} on the (100) steps.[78] The potential region between 0.6 and 0.85 V corresponds to the OH adsorption on (111) terraces, and the asymmetry of the redox peaks indicates irreversible OH adsorption−desorption. In the potential region between 0.85 and 1.0 V, OH_{ad} is progressively transformed into O_{ad}. For the surfaces having n atom-wide (111) terraces and monatomic (100) steps whose Miller indices are Pt(n + 1, n − 1, n − 1), the charge density on the (100) steps is given by the expression according to the hard-sphere model[79]:

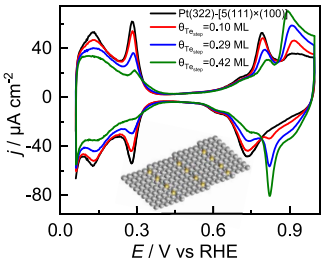

Figure 3. Cyclic voltammograms of Te-modified Pt(322) with different coverages in Ar-saturated 0.1 M $HClO_4$. Scan rate: 50 mV/s. Potential region: 0.06−1.0 V.

$$q_{\text{step}}^{\text{Pt}(n+1,n-1,n-1)} = \frac{q_{\text{Pt}(111)}}{(n-1/3)}\cos(\alpha) \tag{5}$$

where $q_{\text{Pt}(111)}$ is the charge density measured for a process occurring on Pt(111) transferring the 1 e^- per platinum site (241 μC cm^{-2}) and α is the angle between the (hkl) surface and the (111) plane. For the Pt(322) surface, n is equal to 5, $\cos(\alpha)$ is 0.986, and the calculated charge using a hard-sphere model for the step with a H_{ad} coverage equal to 1 is 50.4 μC cm^{-2}. The experimental charge density of species adsorption−desorption at the step sites is obtained by integrating the area of the peaks at 0.2−0.35 V and subtracting appropriate baselines, which are 48.8 μC cm^{-2}. This value is consistent with the expected hard-sphere model value, within the margin of error, thus confirming the electrode's quality.

It has been shown that the initial deposition of the adatom on the step sites or terrace sites depends on the electronegativity of the adatom and substrate atom.[43] The electronegativity of Te is 2.10, which is smaller than that of Pt, 2.28. Therefore, when Te adsorbs on platinum stepped crystal planes, it tends to deposit initially on the lower part of the step to later deposit on the terrace. The charge density under the peak related to the (100) steps diminishes as Te is deposited, whereas the diminution of the signal related to the terraces is very small. In this respect, it should be noted that when Te is deposited on the (111) terraces, a reversible peak at 0.83 V

https://doi.org/10.1021/acscatal.3c04876
ACS Catal. 2023, 13, 16045−16054

should appear, corresponding to the redox processes of the Te adatoms deposited on the (111) terrace.[80] The absence of this peak indicates that the Te adsorption on the (111) terrace sites is highly restricted. Additional changes upon the deposition of Te are also observed in the voltammograms. The onset potential of OH_{ad} on the (111) terraces shifts positively and the total coverage of OH_{ad} decreases with Te coverage, indicating that the presence of Te on the step affects the adsorption of OH on the terrace. With increasing Te coverage, the binding energy between the (111) terraces and OH_{ad} weakens, as evidenced by the positive shift of the onset potential for OH adsorption on the (111) terraces. Also, a new irreversibly peak appears at $E > 0.9$ V, whose charge increases with the Te coverage. The potential of this peak is very similar to that observed for the redox process of Te deposited on the Pt(100), and thus, this peak should be related to the Te deposited on the (100) steps. For the calculation of θ_{Te} used in this work, since Te is mainly deposited on the step sites, the integral area of the peak from 0.2 to 0.35 V is used. Therefore, coverage values refer to the coverages on the step sites. The expression used will be the same as that used for the Pt(100) surface.

The study of the ORR on the Te-modified stepped surfaces is restricted to the Te coverages where Te is only deposited on the step. As the studies with the Pt(111) surface demonstrate, the deposition of Te on the (111) domains does not enhance ORR activity, given that Te is in the oxidized state at $E > 0.83$ V, which is inactive for electrocatalysis. Compared with the significant increase in the activity for Pt(100) induced by Te modification, the enhancement of the ORR activity on the Te-modified Pt(322) electrode is significantly smaller in Figure 4a. Moreover, at potentials higher than the redox peak of Te adatoms on the (100) steps (as marked by the dashed line in Figure 4b), ORR currents at Te-modified electrodes are smaller than that at unmodified Pt(332). At potentials lower than the redox peak of Te adatoms, the ORR current increases

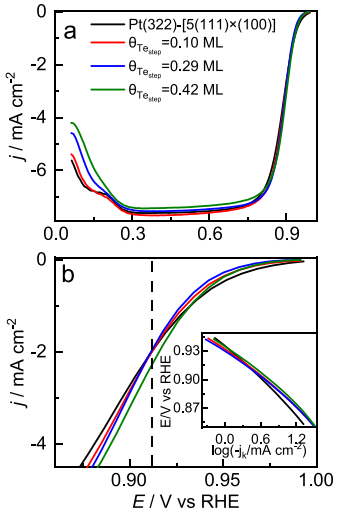

Figure 4. Linear sweep voltammograms for the oxygen reduction reaction on hanging meniscus configuration at 2500 rpm (positive scan direction) in O_2-saturated 0.1 M $HClO_4$ for Te-modified Pt(322) electrodes with different Te coverages at (a) 0.06−1.0 V and (b) 0.87−1.0 V. The dashed vertical line shows the peak potential for the oxidation of the Te adatoms in the positive scan direction. The inset of (b) shows the Tafel plots at different Te coverages on Pt(322). Scan rate: 50 mV/s.

and becomes larger than that of the unmodified Pt(322). This behavior is attributed to the combined effects of the oxidized Te (which is inactive for the ORR) and OH adsorption attenuation on the (111) terrace. A similar conclusion is obtained for the calculated values of j_k. The polarization curves at different rotation rates are given in Figure S1c,d, and there is almost no change in the transferred electrons during the ORR. Additionally, from the Tafel plots of different θ_{Te} of Pt(322)@Te electrodes in the inset of Figure 4b, the curves shift positively compared with the unmodified electrode, and the Tafel slopes are in the range of −50 to −60 mV. Therefore, it can be concluded that the reaction mechanism remains unchanged.

3.3. Trends in ORR Activity with Te Coverage. It is possible to elucidate the chemical nature of the reaction sites by analyzing the changes in the ORR kinetic currents as a function of θ_{Te}. This strategy has previously been used for the ORR on Cu and Br-modified Pt(111) electrodes.[50,81] To accomplish this aim, the ORR on Te-modified platinum single-crystal surfaces is studied further by varying Te coverages, and the results are presented in Figure 5. It is concluded that the

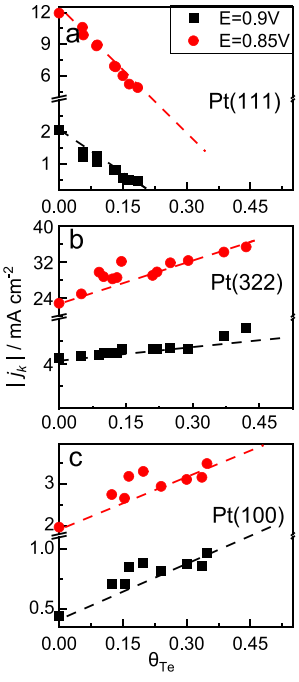

Figure 5. ORR activities (j_k) at 0.9 V (black squares) and 0.85 V(red circles) with different Te coverages on (a) Pt(111), (b) Pt(322), and (c) Pt(100). The obtained currents (j) are from the ORR polarization curve at 2500 rpm and 50 mV/s. The dashed lines provide only a visual guide on the evolution of the activities with the coverage.

ORR activity decreases when Te is adsorbed on the Pt(111) electrode, and the overall ORR activity is enhanced when Te is modified on the Pt stepped surfaces and the Pt(100) electrode. DFT calculations have shown that Te adatoms downshift the d-band center of Pt; this may lead to lower binding energy of the ORR intermediates.[65] The combination of both changes should result in an increase in the ORR activity,[59] as confirmed by the experimental results. For Te-modified Pt(111), Te exists in the oxidized state on Pt(111) (Figure S2a) at the sampling potentials where the activity of the ORR process is analyzed. As the coverage of the oxidized Te increases and blocks more active sites, the activity diminishes due to the

https://doi.org/10.1021/acscatal.3c04876
ACS Catal. 2023, 13, 16045−16054

partial blockage of Pt and the lower activity of the remaining free sites. For Te-modified Pt(100), the ORR activity increases approximately linearly with an increase in Te coverage. Te exists mostly in the reduced state and decreases the OH binding strength. This results in an enhancement of the ORR activity, overcompensating for the diminution in the number of free Pt sites. A Te adatom interacts with 4 Pt atoms, and the number of Pt atoms in the (100) domains that are affected by Te adatom increases with increasing Te coverage. The behavior of the Te-modified Pt(322) electrode is different for the two sampling potentials. At 0.9 V, the activity is almost independent of the Te step coverage for low and intermediate values and slightly increases at higher values. However, at 0.85 V, a significant increase is observed for all of the coverage values. As previously discussed, the peak potential for Te oxidation on the (100) steps is ca. 0.91 V. Consequently, at 0.9 V, a fraction of the Te adatoms is already in their oxidized state, and their contribution to the current enhancement is small. On the other hand, at 0.85 V, Te adatoms are in their reduced state and enhance the activity. It should be noted that the ORR activity of the Pt(322) surface is significantly higher than those of the Pt(111) and Pt(100) electrodes. The increase is attributed to the presence of steps.[82] Despite the partial blockage of the steps caused by the Te adatoms, the activity still increases with the Te coverage. Since Te is initially deposited on the lower part of the step,[43] the activity of the Pt sites adjacent to Te on the step should be very large so that they can compensate for the blockage of the step site.

3.4. Trends in ORR Activity with Step Density. In order to better understand the behavior of Te deposited on the steps and how it modifies the catalytic activity for the ORR, we analyzed additional stepped surfaces with (111) terraces and (100) steps. The CVs and ORR polarization curves of other Pt stepped single-crystal electrodes containing different atom-wide (111) terraces are in the Supporting Information in Figure S3 (Pt(311) − [2(111) × (100)]), Figure S4 (Pt(755) − [6(111) × (100)]), and Figure S5 (Pt(977) − [8(111) × (100)]). The resulting changes in the CVs due to Te deposition on platinum stepped crystal planes, Pt(755) and Pt(977), are similar to that of Pt(322). In this regard, Te first deposits at the lower part of the (100) steps. In contrast, the behavior of Pt(311) is quite different from those of other stepped crystal electrodes because it is the turning point in the series. It can be described as a surface containing 2 atom-wide (111) terraces separated by (100) monatomic steps or 2 atom-wide (100) terraces containing (111) monatomic steps. Starting from 0.06 V, the signals between 0.06 and 0.2 V are related to the H desorption on (111) sites, and the two peaks in the potential region 0.2−0.4 V are related to the H desorption and the OH adsorption on the (100) sites.[78] When Te adsorbs on Pt(311), all the signals diminish, and the two peaks at 0.2−0.4 V merge into one. In addition, a new peak arises around 0.8 V, which is characteristic of the redox process of Te deposited on the (111) sites. Due to the small size of the terrace and the relatively large size of Te, in this case, it is not possible to distinguish between Te deposited on the steps and terrace sites in this case.

The ORR activity of different Pt stepped crystal planes in the $[01\bar{1}]$ zone in Figure 6a is the same as that reported by Feliu[66,83] and Hoshi and co-workers[82] and follows the order as shown in Figure S7: Pt(322)([5(111) × (100)]) > Pt(755) ([6(111) × (100)]) > Pt(977)([8(111) × (100)]) > Pt(111) > Pt(311)([2(111) × (100)]) > Pt(100). Bandrenka

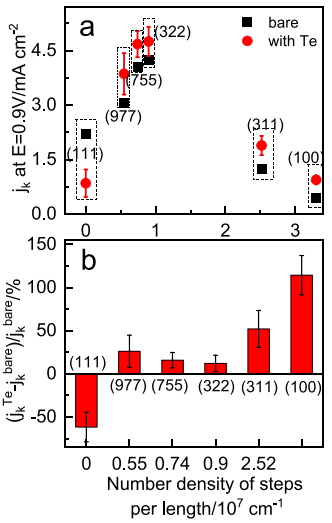

Figure 6. (a) ORR activities (j_k) at 0.9 V on the bare and Te-modified Pt electrodes containing n atom-wide (111) terraces and (100) steps, plotted against the number density of steps per unit length. (b) Enhancement factor of the j_k of Pt(*hkl*)@Te compared with Pt(*hkl*).

attributed the trends of activity with step density to the binding energy of the oxygenated species.[84] Thus, the Pt(111) surface is located on the side of the volcano curve for which OH adsorption energy is too strong, in this case, 0.1 eV, greater than the optimal value.[85] When introducing the (100) steps into the (111) domains, OH_{ad} on the (100) steps interacts with OH_{ad} on the (111) terraces, and then, the hydration network structure between OH_{ad} on the hydrated terrace and the H_2O in the electrolyte is broken. Thus, the ORR activity increases, since it destabilizes OH adsorption. However, this interpretation poses a problem that the ORR activity of the Pt(311) surface, which can be considered a surface with high step density, is lower than that of Pt(111). The terrace width is so short that the adsorption of oxygenated species on the (100) step can interact with those on the (111) terraces. Moreover, due to the Smoluchowski effect,[86] which implies an electron density redistribution over the step, the energetics of the different sites tend to converge, thereby diminishing the differences between them. This problem is absent in the Pt-stepped single-crystal electrodes with relatively long (111) terraces, such as Pt(322), Pt(755), and Pt(977), and thus, the step reduces the OH adsorption energy on (111) terraces. For this reason, the Pt(322) electrode is the most active of all the stepped crystal planes used in the present study.

As for the oxygen reduction reaction on the Te-modified electrodes, an enhanced ORR activity is observed for all of the Pt stepped surfaces. More specifically, the onset and half-wave potentials of Pt(311) shift noticeably to higher values. On the other hand, for the surfaces with a low step density, that is, Pt(322), Pt(755), and Pt(977), the enhancement is less significant. Nevertheless, the maximum activity is still present in the Pt(322) electrode, and the activity order is consistent with that of the unmodified electrodes. When calculating the relative enhancement of the current due to the modification of Te (see Figure 6b), we observe the maximum improvement in the activity in Pt(100), with about 134% increase in kinetic current at 0.9 V. Leaving aside the Pt(111) electrode, because the Te adatoms would only increase their activity at $E < 0.8$ V, when the adatoms are in the reduced state on Pt(111), for the

https://doi.org/10.1021/acscatal.3c04876
ACS Catal. 2023, 13, 16045−16054

remaining sites, a positive effect is observed. For the Te-modified Pt stepped surfaces, the enhancement ratio diminishes as the step density increases up to the Pt(322) electrode. The activity for these surfaces can be considered as an averaged contribution of the step and terrace sites, in which the activity of the step sites is significantly larger than that of the terrace sites. Since the presence of Te adsorbed on the steps only increases the activity of the terrace sites, it would be expected that the higher the step density, the higher the relative activity increases. However, this is not the case, since for the Pt(322) electrode, the relative increase is the smallest for the whole series of stepped surfaces. This fact implies that other effects, not related to the electronic modification of the surfaces, are affecting the behavior. In this sense, the modification of the water structure near the adatom may also play a role. Thus, the disruption of this water structure brought about by the presence of steps on the (111) terraces may be intensified in the case of the surfaces with long terraces. For surfaces with short terraces, the addition of Te adatoms on the steps does not increase this process because the adlayer is already fully disrupted. However, the behaviors of the Pt(311) and Pt(100) electrodes are similar. On these surfaces, the relative enhancement is larger and all the sites participate in the enhancement. Chronoamperometry was also used to determine the stability of the ORR catalytic activity and structure-sensitive effects. Figure S8 shows that Te modification can slow the decay of ORR current and enhance the ORR activity of Pt electrodes by the currents at 0.9 and 0.85 V. However, the current of the Te-modified Pt(322) is initially smaller than that of Pt(322) for the first 10 s but then increases rapidly when applying potential at 0.9 V. This phenomenon is probably associated with the oxidation state of Te. In the beginning, Te exists mostly in the oxidized state and then gradually changes to the reduced state and enhances the ORR activity, which agrees with the previous conclusions.

3.5. Voltammetric Behavior of Te-Modified Pt(*hkl*) Electrodes after ORR. For practical applications, it is important to establish the stability of the Te adatoms under operative conditions. Therefore, the CVs of Te-modified platinum electrodes before and after ORR in the supporting electrolyte are displayed in Figure 7. It is evident that CVs of Te-modified Pt(111) and Pt(100) show a diminution of the amount of Te adsorbed on the surface after the ORR. Conversely, this diminution is less significant for the Te-modified Pt(322) surface. In Figure 7a for Pt(111), it is evident that the peak current at 0.83 V decreases after ORR, indicating partial desorption of Te from the surface during the ORR experiments. This may be due to the instability of Te in the presence of oxygen and the sweep to high potentials (1 V). In addition, Te interacts weakly with the closely packed Pt(111) surface, as seen from the longer Pt−Te bond length compared with that of Pt(100) by DFT calculations.[65] There is a strong interaction between Pt(100) and adsorbed Te. However, the desorption of Te from the Pt(100) surface is also observed, as demonstrated by the reduced area of the Te redox peak at 0.9−1.0 V in Figure 7c. This phenomenon may be due to the instability of Te in the presence of oxygen and surface disorder during ORR. In contrast, the changes in the CV of Te-modified Pt (322) after ORR are significantly smaller. As mentioned before, the most favorable site for Te deposition is the step site, which stabilizes the adatom on this site and impedes Te desorption. Therefore, Te modification on the (100) step sites can protect low-coordinated sites from reconstruction and enhance the stability of the surface structure of Pt(*hkl*)@Te.

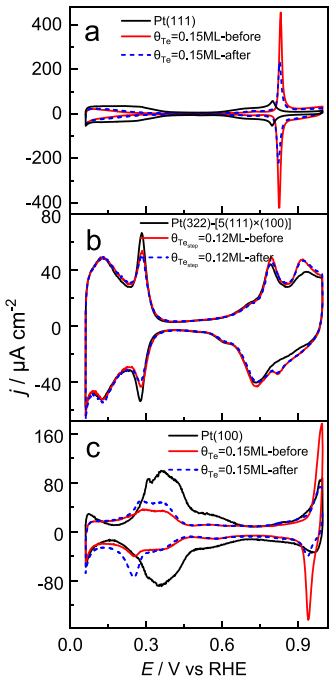

Figure 7. Cyclic voltammograms of Te-modified (a) Pt(111), (b) Pt(322), and (c) Pt(100) in Ar-saturated 0.1 M $HClO_4$. The red solid line and blue dashed line indicate the CVs of Te-modified Pt(*hkl*) recorded before ORR and after ORR, respectively. Scan rate: 50 mV/s. Potential region: 0.06−1.0 V.

4. CONCLUSIONS

A series of platinum stepped crystal electrodes containing different (111) atom terrace widths and (100) monatomic steps modified by tellurium has been used to study the effects of Te modification on the ORR performance. Except for Pt(111), all other surfaces display enhanced ORR activity with Te modification. Besides, the Pt(322) electrode has the best ORR activity, and the Pt(100) electrode has the largest ORR activity enhancement factor. The improvement of the ORR activity can be related to the intermediate binding energy and the state of Te. These results imply that the modification of Pt with species that transfer electrons to Pt can be an efficient strategy to enhance its ORR activity and stability. The results presented here indicate that the presence of Te enhances the ORR provided that Te is in its reduced state; that is, OH is not adsorbed on the Te adatoms. The charge transfer from Te to the Pt surface results in less favorable OH adsorption. Since the OH desorption is the RDS in the ORR mechanism, a catalytic effect is observed. However, the oxidation of the Te adatoms, which implies the adsorption of OH, deactivates the positive effect, probably due to the reordering of the water adlayer around the adatoms. Thus, elements that could transfer charge to the Pt electrode and destabilize OH adsorption can have a positive impact on the electrocatalysis of the ORR, provided that they do not modify the water structure by adsorbing OH on them, which may pave the way for further evolution of Pt-based catalysts for PEFCs. In this respect, further efforts in the characterization of submonolayer amounts of foreign metals deposited on surfaces are required to fully understand their effect on the ORR.

https://doi.org/10.1021/acscatal.3c04876
ACS Catal. 2023, 13, 16045−16054

■ ASSOCIATED CONTENT

Supporting Information

The Supporting Information is available free of charge at https://pubs.acs.org/doi/10.1021/acscatal.3c04876.

The following files are available free of charge. ORR polarization curves of bare and Te-modified Pt(100) and Pt(322) at different rotation rates; voltammetric behavior and ORR activity of Te-modified Pt surfaces in [01$\bar{1}$] region; ORR polarization curves in hanging meniscus Pt(*hkl*) in [01$\bar{1}$] region; and chronoamperometric behavior of bare and Te-modified Pt(*hkl*) (PDF)

■ AUTHOR INFORMATION

Corresponding Authors

Yan-Xia Chen − *Hefei National Research Center for Physical Sciences at Microscale, Department of Chemical Physics, University of Science and Technology of China, Hefei 230026, China;* orcid.org/0000-0002-1370-7422; Email: yachen@ustc.edu.cn

Enrique Herrero − *Instituto de Electroquímica, Universidad de Alicante, Alicante E-03080, Spain;* orcid.org/0000-0002-4509-9716; Email: herrero@ua.es

Authors

Ting-Ting Mao − *Hefei National Research Center for Physical Sciences at Microscale, Department of Chemical Physics, University of Science and Technology of China, Hefei 230026, China*

Zhen Wei − *Hefei National Research Center for Physical Sciences at Microscale, Department of Chemical Physics, University of Science and Technology of China, Hefei 230026, China*

Bing-Yu Liu − *Hefei National Research Center for Physical Sciences at Microscale, Department of Chemical Physics, University of Science and Technology of China, Hefei 230026, China*

Yu-Jun Xu − *Hefei National Research Center for Physical Sciences at Microscale, Department of Chemical Physics, University of Science and Technology of China, Hefei 230026, China*

Jun Cai − *Hefei National Research Center for Physical Sciences at Microscale, Department of Chemical Physics, University of Science and Technology of China, Hefei 230026, China*

Juan M. Feliu − *Instituto de Electroquímica, Universidad de Alicante, Alicante E-03080, Spain;* orcid.org/0000-0003-4751-3279

Complete contact information is available at: https://pubs.acs.org/10.1021/acscatal.3c04876

Author Contributions

The manuscript was written through the contributions of all authors. All authors have given approval to the final version of the manuscript.

Funding

This work was supported by the National Natural Science Foundation of China (No. 22172151, 21972131, and 21832004). E.H. gratefully acknowledged the International Professorship by USTC and financial support from the Ministerio de Ciencia e Innovación (project PID2022−137350NB-I00).

Notes

The authors declare no competing financial interest.

■ ACKNOWLEDGMENTS

The authors thank Prof. Zhi-Feng Liu, Prof. Jun Huang and Wei Chen for the invaluable discussion.

■ ABBREVIATIONS

ORR	oxygen reduction reaction
RHE	reversible hydrogen electrode
CV	cyclic voltammograms
HMRDE	hanging meniscus rotation disk electrode
PZFC	potential of zero free charge

■ REFERENCES

(1) Debe, M. K. Electrocatalyst approaches and challenges for automotive fuel cells. *Nature* **2012**, *486* (7401), 43−51.

(2) Wang, X. X.; Swihart, M. T.; Wu, G. Achievements, challenges and perspectives on cathode catalysts in proton exchange membrane fuel cells for transportation. *Nature Catalysis* **2019**, *2* (7), 578−589.

(3) Jiao, K.; Xuan, J.; Du, Q.; Bao, Z.; Xie, B.; Wang, B.; Zhao, Y.; Fan, L.; Wang, H.; Hou, Z.; Huo, S.; Brandon, N. P.; Yin, Y.; Guiver, M. D. Designing the next generation of proton-exchange membrane fuel cells. *Nature* **2021**, *595* (7867), 361−369.

(4) Nørskov, J. K.; Rossmeisl, J.; Logadottir, A.; Lindqvist, L.; Kitchin, J. R.; Bligaard, T.; Jónsson, H. Origin of the Overpotential for Oxygen Reduction at a Fuel-Cell Cathode. *J. Phys. Chem. B* **2004**, *108* (46), 17886−17892.

(5) Chen, W.; Huang, J.; Wei, J.; Zhou, D.; Cai, J.; He, Z. D.; Chen, Y. X. Origins of high onset overpotential of oxygen reduction reaction at Pt-based electrocatalysts: A mini review. *Electrochem. Commun.* **2018**, *96*, 71−76.

(6) Liu, B. Y.; Chen, W.; Ye, X. X.; Cai, J.; Chen, Y. X. IrO_2 as a promising support to boost oxygen reduction reaction on Pt in acid under high temperature conditions. *J. Chem. Phys.* **2023**, *158* (13), 134710.

(7) Zhou, D.; Zheng, Y. L.; Ze, H.; Ye, X.; Cai, J.; Chen, Y. X.; Tian, Z. Q. Why Does Pt Shell Bearing Tensile Strain Still Have Superior Activity for the Oxygen Reduction Reaction? *J. Phys. Chem. C* **2022**, *126* (42), 17913−17922.

(8) Maley, M.; Hill, J. W.; Saha, P.; Walmsley, J. D.; Hill, C. M. The Role of Heating in the Electrochemical Response of Plasmonic Nanostructures under Illumination. *J. Phys. Chem. C* **2019**, *123* (19), 12390−12399.

(9) Chen, W.; Cui, H. W.; Liao, L. W.; Xu, Y. J.; Cai, J.; Chen, Y. X. Challenges in Unravelling the Intrinsic Kinetics of Gas Reactions at Rotating Disk Electrodes by Koutecky−Levich Equation. *J. Phys. Chem. C* **2023**, *127* (33), 16235−16248.

(10) Chen, W.; Zhang, L. L.; Wei, Z.; Zhang, M. K.; Cai, J.; Chen, Y. X. The electrostatic effect and its role in promoting electrocatalytic reactions by specifically adsorbed anions. *Phys. Chem. Chem. Phys.* **2023**, *25* (12), 8317−8330.

(11) Clavilier, J.; Armand, D.; Sun, S. G.; Petit, M. Electrochemical adsorption behaviour of platinum stepped surfaces in sulphuric acid solutions. *Journal of Electroanalytical Chemistry and Interfacial Electrochemistry* **1986**, *205* (1−2), 267−277.

(12) Feliu, J. M.; Llorca, M. J.; Gómez, R.; Aldaz, A. Electrochemical behaviour of irreversibly adsorbed tellurium dosed from solution on Pt(h, k, l) single crystal electrodes in sulphuric and perchloric acid media. *Surf. Sci.* **1993**, *297* (2), 209−222.

(13) Tripković, V.; Skúlason, E.; Siahrostami, S.; Nørskov, J. K.; Rossmeisl, J. The oxygen reduction reaction mechanism on Pt(111) from density functional theory calculations. *Electrochim. Acta* **2010**, *55* (27), 7975−7981.

(14) Li, M. F.; Liao, L. W.; Yuan, D. F.; Mei, D.; Chen, Y. X. pH effect on oxygen reduction reaction at Pt(111) electrode. *Electrochim. Acta* **2013**, *110*, 780−789.

(15) Mei, D.; He, Z. D.; Zheng, Y. L.; Jiang, D. C.; Chen, Y. X. Mechanistic and kinetic implications on the ORR on a Au(100)

electrode: pH, temperature and H-D kinetic isotope effects. *Phys. Chem. Chem. Phys.* **2014**, *16* (27), 13762−13773.
(16) Liao, L. W.; Zheng, Y. L.; Wei, J.; Chen, Y. X. O_2 surface concentration change and its implication on oxygen reduction mechanism and kinetics at platinum in acidic media. *Electrochem. Commun.* **2015**, *58*, 73−75.
(17) Zhang, L.; Cai, J.; Chen, Y.; Huang, J. Modelling electrocatalytic reactions with a concerted treatment of multistep electron transfer kinetics and local reaction conditions. *J. Phys.: Condens. Matter* **2021**, *33* (50), 504002.
(18) Li, Y.; Chen, Y. X.; Liu, Z. F. OH^-...Au Hydrogen Bond and Its Effect on the Oxygen Reduction Reaction on Au(100) in Alkaline Media. *J. Phys. Chem. Lett.* **2022**, *13* (39), 9035−9043.
(19) Herrero, E.; Feliu, J. M. Understanding formic acid oxidation mechanism on platinum single crystal electrodes. *Current Opinion in Electrochemistry* **2018**, *9*, 145−150.
(20) Wei, Z.; Jordá-Faus, P.; Chico-Mesa, L.; Cai, J.; Chen, Y. X.; Rodes, A.; Feliu, J. M.; Herrero, E. Formic acid oxidation on different coverages of Bismuth-modified Pt(100): A detailed Voltammetric and FTIR study. *J. Catal.* **2023**, *426*, 61−70.
(21) Chen, X.; Granda-Marulanda, L. P.; McCrum, I. T.; Koper, M. T. M. Adsorption processes on a Pd monolayer-modified Pt(111) electrode. *Chem. Sci.* **2020**, *11* (6), 1703−1713.
(22) Mayrhofer, K. J. J.; Strmcnik, D.; Blizanac, B. B.; Stamenkovic, V.; Arenz, M.; Markovic, N. M. Measurement of oxygen reduction activities via the rotating disc electrode method: From Pt model surfaces to carbon-supported high surface area catalysts. *Electrochim. Acta* **2008**, *53* (7), 3181−3188.
(23) Chen, Q. S.; Vidal-Iglesias, F. J.; Solla-Gullón, J.; Sun, S. G.; Feliu, J. M. Role of surface defect sites: from Pt model surfaces to shape-controlled nanoparticles. *Chem. Sci.* **2012**, *3* (1), 136−147.
(24) Kodama, K.; Nagai, T.; Kuwaki, A.; Jinnouchi, R.; Morimoto, Y. Challenges in applying highly active Pt-based nanostructured catalysts for oxygen reduction reactions to fuel cell vehicles. *Nat. Nanotechnol* **2021**, *16* (2), 140−147.
(25) McCrum, I. T.; Koper, M. T. M. The role of adsorbed hydroxide in hydrogen evolution reaction kinetics on modified platinum. *Nature Energy* **2020**, *5* (11), 891−899.
(26) Rizo, R.; Melle, G.; Herrero, E.; Feliu, J. M. Foreign adatoms on well-defined platinum electrodes: catalytic activity. *In Reference Module in Chemistry, Molecular Sciences and Chemical Engineering* **2024**, 278−288.
(27) Kodama, K.; Jinnouchi, R.; Takahashi, N.; Murata, H.; Morimoto, Y. Activities and Stabilities of Au-Modified Stepped-Pt Single-Crystal Electrodes as Model Cathode Catalysts in Polymer Electrolyte Fuel Cells. *J. Am. Chem. Soc.* **2016**, *138* (12), 4194−4200.
(28) Stephens, I. E.; Bondarenko, A. S.; Perez-Alonso, F. J.; Calle-Vallejo, F.; Bech, L.; Johansson, T. P.; Jepsen, A. K.; Frydendal, R.; Knudsen, B. P.; Rossmeisl, J.; Chorkendorff, I. Tuning the activity of Pt(111) for oxygen electroreduction by subsurface alloying. *J. Am. Chem. Soc.* **2011**, *133* (14), 5485−5491.
(29) Hernandez-Fernandez, P.; Masini, F.; McCarthy, D. N.; Strebel, C. E.; Friebel, D.; Deiana, D.; Malacrida, P.; Nierhoff, A.; Bodin, A.; Wise, A. M.; Nielsen, J. H.; Hansen, T. W.; Nilsson, A.; Stephens, I. E.; Chorkendorff, I. Mass-selected nanoparticles of Pt_xY as model catalysts for oxygen electroreduction. *Nat. Chem.* **2014**, *6* (8), 732−738.
(30) Stamenkovic, V. R.; Fowler, B.; Mun, B. S.; Wang, G.; Ross, P. N.; Lucas, C. A.; Markovic, N. M. Improved oxygen reduction activity on $Pt_3Ni(111)$ via increased surface site availability. *Science* **2007**, *315* (5811), 493−497.
(31) Zhang, J.; Mo, Y.; Vukmirovic, M. B.; Klie, R.; Sasaki, K.; Adzic, R. R. Platinum Monolayer Electrocatalysts for O_2 Reduction: Pt Monolayer on Pd(111) and on Carbon-Supported Pd Nanoparticles. *J. Phys. Chem. B* **2004**, *108* (30), 10955−10964.
(32) Adzic, R. R.; Zhang, J.; Sasaki, K.; Vukmirovic, M. B.; Shao, M.; Wang, J. X.; Nilekar, A. U.; Mavrikakis, M.; Valerio, J. A.; Uribe, F. Platinum Monolayer Fuel Cell Electrocatalysts. *Top. Catal.* **2007**, *46* (3−4), 249−262.
(33) Abe, T.; Swain, G. M.; Sashikata, K.; Itaya, K. Effect of underpotential deposition (UPD) of copper on oxygen reduction at Pt(111) surfaces. *J. Electroanal. Chem.* **1995**, *382* (1−2), 73−83.
(34) Herrero, E.; Buller, L. J.; Abruna, H. D. underpotential deposition at single crystal surfaces of Au, Pt Ag and other materials. *Chem. Rev.* **2001**, *101* (7), 1897−1930.
(35) Perales-Rondon, J. V.; Ferre-Vilaplana, A.; Feliu, J. M.; Herrero, E. Oxidation mechanism of formic acid on the bismuth adatom-modified Pt(111) surface. *J. Am. Chem. Soc.* **2014**, *136* (38), 13110−13113.
(36) Boronat-González, A.; Herrero, E.; Feliu, J. M. Fundamental aspects of HCOOH oxidation at platinum single crystal surfaces with basal orientations and modified by irreversibly adsorbed adatoms. *J. Solid State Electrochem.* **2014**, *18* (5), 1181−1193.
(37) Figueiredo, M. C.; Vidal-Iglesias, F.; Solla-Gullón, J.; Climent, V.; Feliu, J. M. Nitrate Reduction on Platinum (111) Surfaces Modifiedl with Bi: Single Crystalsl and Nanoparticles. *Zeitschrift für Physikalische Chemie* **2012**, *226* (9−10), 901−917.
(38) Kwon, Y.; Hersbach, T. J. P.; Koper, M. T. M. Electro-Oxidation of Glycerol on Platinum Modified by adatoms: Activity and Selectivity Effects. *Top. Catal.* **2014**, *57* (14−16), 1272−1276.
(39) Wei, Z.; Yu, A.; Gisbert-González, J. M.; Cai, J.; Chen, Y. X.; Feliu, J. M.; Herrero, E. Mechanism of formic acid oxidation on Bi modified Pt(111): Implication from the concentration effect of formic acid and different coverages of Bi. *Electrochim. Acta* **2023**, *449*, No. 142188.
(40) Perales-Rondón, J. V.; Busó-Rogero, C.; Solla-Gullón, J.; Herrero, E.; Feliu, J. M. Formic acid electrooxidation on thallium modified platinum single crystal electrodes. *J. Electroanal. Chem.* **2017**, *800*, 82−88.
(41) Del Colle, V.; Souza-Garcia, J.; Tremiliosi-Filho, G.; Herrero, E.; Feliu, J. M. Electrochemical and spectroscopic studies of ethanol oxidation on Pt stepped surfaces modified by tin adatoms. *Phys. Chem. Chem. Phys.* **2011**, *13* (26), 12163−12172.
(42) Hazzazi, O. A.; Attard, G. A.; Wells, P. B.; Vidal-Iglesias, F. J.; Casadesus, M. Electrochemical characterisation of gold on Pt{hkl} for ethanol electrocatalysis. *J. Electroanal. Chem.* **2009**, *625* (2), 123−130.
(43) Herrero, E.; Climent, V. C.; Feliu, J. M. On the different adsorption behavior of bismuth, sulfur, selenium and tellurium on a Pt(775) stepped surface. *Electrochem. Commun.* **2000**, *2* (9), 636−640.
(44) Brankovic, S. R.; Wang, J. X.; Adžić, R. R. Metal monolayer deposition by replacement of metal adlayers on electrode surfaces. *Surf. Sci.* **2001**, *474* (1−3), L173−L179.
(45) Yang, C. L.; Wang, L. N.; Yin, P.; Liu, J.; Chen, M. X.; Yan, Q. Q.; Wang, Z. S.; Xu, S. L.; Chu, S. Q.; Cui, C.; Ju, H.; Zhu, J.; Lin, Y.; Shui, J.; Liang, H. W. Sulfur-anchoring synthesis of platinum intermetallic nanoparticle catalysts for fuel cells. *Science* **2021**, *374* (6566), 459−464.
(46) Sun, Y.; Polani, S.; Luo, F.; Ott, S.; Strasser, P.; Dionigi, F. Advancements in cathode catalyst and cathode layer design for proton exchange membrane fuel cells. *Nat. Commun.* **2021**, *12* (1), 5984.
(47) Greeley, J.; Stephens, I. E.; Bondarenko, A. S.; Johansson, T. P.; Hansen, H. A.; Jaramillo, T. F.; Rossmeisl, J.; Chorkendorff, I.; Norskov, J. K. Alloys of platinum and early transition metals as oxygen reduction electrocatalysts. *Nat. Chem.* **2009**, *1* (7), 552−556.
(48) Stephens, I. E. L.; Bondarenko, A. S.; Grønbjerg, U.; Rossmeisl, J.; Chorkendorff, I. Understanding the electrocatalysis of oxygen reduction on platinum and its alloys. *Energy Environ. Sci.* **2012**, *5* (5), 6744−6762.
(49) Tang, M.; Zhang, S.; Chen, S. Pt utilization in proton exchange membrane fuel cells: structure impacting factors and mechanistic insights. *Chem. Soc. Rev.* **2022**, *51* (4), 1529−1546.
(50) Tymoczko, J.; Calle-Vallejo, F.; Colic, V.; Koper, M. T. M.; Schuhmann, W.; Bandarenka, A. S. Oxygen Reduction at a Cu-Modified Pt(111) Model Electrocatalyst in Contact with Nafion Polymer. *ACS Catal.* **2014**, *4* (10), 3772−3778.
(51) Zhang, J.; Vukmirovic, M. B.; Xu, Y.; Mavrikakis, M.; Adzic, R. R. Controlling the Catalytic Activity of Platinum-Monolayer Electro-

https://doi.org/10.1021/acscatal.3c04876
ACS Catal. 2023, 13, 16045−16054

catalysts for Oxygen Reduction with Different Substrates. *Angew. Chem.* **2005**, *117* (14), 2170−2173.
(52) Miyabayashi, K.; Nishihara, H.; Miyake, M. Platinum nanoparticles modified with alkylamine derivatives as an active and stable catalyst for oxygen reduction reaction. *Langmuir* **2014**, *30* (10), 2936−2942.
(53) Saikawa, K.; Nakamura, M.; Hoshi, N. Structural effects on the enhancement of ORR activity on Pt single-crystal electrodes modified with alkylamines. *Electrochem. Commun.* **2018**, *87*, 5−8.
(54) Kumeda, T.; Tajiri, H.; Sakata, O.; Hoshi, N.; Nakamura, M. Effect of hydrophobic cations on the oxygen reduction reaction on singlecrystal platinum electrodes. *Nat. Commun.* **2018**, *9* (1), 4378.
(55) Li, Y.; Hart, J.; Profitt, L.; Intikhab, S.; Chatterjee, S.; Taheri, M.; Snyder, J. Sequential Capacitive Deposition of Ionic Liquids for Conformal Thin Film Coatings on Oxygen Reduction Reaction Electrocatalysts. *ACS Catal.* **2019**, *9* (10), 9311−9316.
(56) Wada, N.; Nakamura, M.; Hoshi, N. Structural Effects on the Oxygen Reduction Reaction on Pt Single-Crystal Electrodes Modified with Melamine. *Electrocatalysis* **2020**, *11* (3), 275−281.
(57) Yamazaki, S. I.; Asahi, M.; Taguchi, N.; Ioroi, T.; Kishimoto, Y.; Daimon, H.; Inaba, M.; Koga, K.; Kurose, Y.; Inoue, H. Creation of a Highly Active Pt/Pd/C Core−Shell-Structured Catalyst by Synergistic Combination of Intrinsically High Activity and Surface Decoration with Melamine or Tetra-(tert-butyl)-tetraazaporphyrin. *ACS Catal.* **2020**, *10* (24), 14567−14580.
(58) Gomez-Marin, A. M.; Briega-Martos, V.; Feliu, J. M. Structure effects on electrocatalysts. Oxygen reduction on Te-modified Pt(111) surfaces: Site-blocking vs electronic effects. *J. Chem. Phys.* **2020**, *152* (13), 134702.
(59) Hammer, B.; Nørskov, J. K. Electronic factors determining the reactivity of metal surfaces. *Surf. Sci.* **1995**, *343* (3), 211−220.
(60) Chen, J. Q.; Ye, X. X.; Liao, L. W.; Wei, Z.; Xu, M. L.; Chen, Y. X. Ohmic Drop Compensation in Electrochemical Measurement. *J. Electrochem.* **2021**, *27* (3), 291−300.
(61) Korzeniewski, C.; Climent, V.; Feliu, J. M. *Electrochemistry at Platinum Single Crystal Electrodes*; Taylor & Francis, 2012, *58*, 75−170.
(62) Kibler, L. A.; Cuesta, A.; Kleinert, M.; Kolb, D. M. In-situ STM characterisation of the surface morphology of platinum single crystal electrodes as a function of their preparation. *J. Electroanal. Chem.* **2000**, *484* (1), 73−82.
(63) Arán-Ais, R. M.; Figueiredo, M. C.; Vidal-Iglesias, F. J.; Climent, V.; Herrero, E.; Feliu, J. M. On the behavior of the Pt(100) and vicinal surfaces in alkaline media. *Electrochim. Acta* **2011**, *58*, 184−192.
(64) Herrero, E.; Llorca, M. J.; Feliu, J. M.; Aldaz, A. Oxidation of formic acid on Pt(100) electrodes modified by irreversibly adsorbed tellurium. *J. Electroanal. Chem.* **1995**, *383* (1−2), 145−154.
(65) Koverga, A. A.; Flórez, E.; Gómez-Marín, A. M. Electronic changes at the platinum interface induced by bismuth and tellurium adatom adsorption. *Appl. Surf. Sci.* **2023**, *608*, No. 155137.
(66) Maciá, M. D.; Campiña, J. M.; Herrero, E.; Feliu, J. M. On the kinetics of oxygen reduction on platinum stepped surfaces in acidic media. *J. Electroanal. Chem.* **2004**, *564*, 141−150.
(67) Xu, M. L.; Chen, W.; Liao, L. W.; Wei, Z.; Cai, J.; Chen, Y. X. Identifying diffusion limiting current to unravel the intrinsic kinetics of electrode reactions affected by mass transfer at rotating disk electrode. *Chinese Journal of Chemical Physics* **2022**, *35* (5), 797−804.
(68) Briega-Martos, V.; Herrero, E.; Feliu, J. M. The inhibition of hydrogen peroxide reduction at low potentials on Pt(111): Hydrogen adsorption or interfacial charge? *Electrochem. Commun.* **2017**, *85*, 32−35.
(69) Briega-Martos, V.; Herrero, E.; Feliu, J. M. Recent progress on oxygen and hydrogen peroxide reduction reactions on Pt single crystal electrodes. *Chinese Journal of Catalysis* **2020**, *41* (5), 732−738.
(70) Gómez, R.; Climent, V.; Feliu, J. M.; Weaver, M. J. Dependence of the Potential of Zero Charge of Stepped Platinum (111) Electrodes on the Oriented Step-Edge Density: Electrochemical Implications and Comparison with Work Function Behavior. *J. Phys. Chem. B* **2000**, *104* (3), 597−605.
(71) Sitta, E.; Gómez-Marín, A. M.; Aldaz, A.; Feliu, J. M. Electrocatalysis of H_2O_2 reduction/oxidation at model platinum surfaces. *Electrochem. Commun.* **2013**, *33*, 39−42.
(72) Martínez-Hincapié, R.; Sebastián-Pascual, P.; Climent, V.; Feliu, J. M. Investigating interfacial parameters with platinum single crystal electrodes. *Russian Journal of Electrochemistry* **2017**, *53* (3), 227−236.
(73) Climent, V.; García-Araez, N.; Herrero, E.; Feliu, J. Potential of zero total charge of platinum single crystals: A local approach to stepped surfaces vicinal to Pt(111). *Russian Journal of Electrochemistry* **2006**, *42* (11), 1145−1160.
(74) Ferre-Vilaplana, A.; Perales-Rondón, J. V.; Feliu, J. M.; Herrero, E. Understanding the Effect of the adatoms in the Formic Acid Oxidation Mechanism on Pt(111) Electrodes. *ACS Catal.* **2015**, *5* (2), 645−654.
(75) Karlberg, G. S.; Rossmeisl, J.; Norskov, J. K. Estimations of electric field effects on the oxygen reduction reaction based on the density functional theory. *Phys. Chem. Chem. Phys.* **2007**, *9* (37), 5158−5161.
(76) Yang, Y.; Agarwal, R. G.; Hutchison, P.; Rizo, R.; Soudackov, A. V.; Lu, X.; Herrero, E.; Feliu, J. M.; Hammes-Schiffer, S.; Mayer, J. M.; Abruna, H. D. Inverse kinetic isotope effects in the oxygen reduction reaction at platinum single crystals. *Nat. Chem.* **2023**, *15* (2), 271−277.
(77) Huang, J.; Malek, A.; Zhang, J.; Eikerling, M. H. Non-monotonic Surface Charging Behavior of Platinum: A Paradigm Change. *J. Phys. Chem. C* **2016**, *120* (25), 13587−13595.
(78) Rizo, R.; Fernandez-Vidal, J.; Hardwick, L. J.; Attard, G. A.; Vidal-Iglesias, F. J.; Climent, V.; Herrero, E.; Feliu, J. M. Investigating the presence of adsorbed species on Pt steps at low potentials. *Nat. Commun.* **2022**, *13* (1), 2550.
(79) Clavilier, J.; El Achi, K.; Rodes, A. In situ probing of step and terrace sites on Pt(S)-[n(111) × (111)] electrodes. *Chem. Phys.* **1990**, *141* (1), 1−14.
(80) Rodriguez, P.; Herrero, E.; Aldaz, A.; Feliu, J. M. Tellurium adatoms as an in-situ surface probe of (111) two-dimensional domains at platinum surfaces. *Langmuir* **2006**, *22* (25), 10329−10337.
(81) Marković, N. M.; Gasteiger, H. A.; Grgur, B. N.; Ross, P. N. Oxygen reduction reaction on Pt(111): effects of bromide. *J. Electroanal. Chem.* **1999**, *467* (1−2), 157−163.
(82) Hitotsuyanagi, A.; Nakamura, M.; Hoshi, N. Structural effects on the activity for the oxygen reduction reaction on n(111)−(100) series of Pt: correlation with the oxide film formation. *Electrochim. Acta* **2012**, *82*, 512−516.
(83) Gómez-Marín, A. M.; Rizo, R.; Feliu, J. M. Oxygen reduction reaction at Pt single crystals: a critical overview. *Catalysis Science & Technology* **2014**, *4* (6), 1685−1698.
(84) Bandarenka, A. S.; Hansen, H. A.; Rossmeisl, J.; Stephens, I. E. Elucidating the activity of stepped Pt single crystals for oxygen reduction. *Phys. Chem. Chem. Phys.* **2014**, *16* (27), 13625−13629.
(85) Viswanathan, V.; Hansen, H. A.; Rossmeisl, J.; Nørskov, J. K. Universality in Oxygen Reduction Electrocatalysis on Metal Surfaces. *ACS Catal.* **2012**, *2* (8), 1654−1660.
(86) Smoluchowski, R. Anisotropy of the Electronic Work Function of Metals. *Phys. Rev.* **1941**, *60* (9), 661−674.

https://doi.org/10.1021/acscatal.3c04876
ACS Catal. 2023, 13, 16045−16054